

Quasiequilibrium distribution function of anisotropic phonon systems and the interaction of pulses of low-energy phonons in superfluid helium

I. N. Adamenko,^{1,2} Yu. A. Kitsenko,¹ K. E. Nemchenko,¹ V. A. Slipko,¹ and A. F. G. Wyatt³

¹Karazin Kharkov National University, Svobody Sq. 4, Kharkov, 61077, Ukraine

²Electro-Physical Scientific and Technical Centre, Chernyshevsky St. 28, Kharkov, 61002, Ukraine

³School of Physics, University of Exeter, Exeter EX4 4QL, United Kingdom

(Received 29 April 2004; revised manuscript received 3 May 2005; published 4 August 2005)

The phenomenon of a hot line forming in liquid helium was observed in experiments carried out in the University of Exeter (UK). It arises when two phonon pulses interact and this is theoretically investigated in this paper. To develop the theory we start from the exact quasiequilibrium distribution function that describes anisotropic phonon systems such as a phonon pulse in superfluid helium. This is related to the approximate distribution function, which is more physically intuitive and was used earlier. The local equilibrium distribution function for phonons in the region of a hot line is obtained from the distribution functions for the phonons in the two interacting pulses. In order to explain the results of experiments, we analyze the effect of different pressures when the angle between the two moving pulses in superfluid helium is constant and also the effect of different angles at the saturated vapor pressure. The conditions suitable for the creation of a hot line are found. The results of the calculations are compared with the experimental data.

DOI: [10.1103/PhysRevB.72.054507](https://doi.org/10.1103/PhysRevB.72.054507)

PACS number(s): 67.40.-w, 62.60.+v, 67.90.+z

I. INTRODUCTION

The phenomenon of a hot line forming in liquid helium was reported in Refs. 1 and 2. It arises when two phonon pulses interact. In this paper we consider anisotropic phonon systems such as a phonon pulse in superfluid helium. We consider an equation for the quasiequilibrium distribution function of anisotropic phonon systems and then analyze the interaction between two phonon pulses that overlap in space. Both these problems involve the scattering between phonons that depends on the phonon dispersion curve—the relation between the phonon energy ε and its momentum p . We write this as

$$\varepsilon = cp(1 + \psi_p), \quad (1)$$

where c is a sound velocity of He II, and $\psi_p = \psi(p)$ is a function that depends on p and describes the deviation of the dispersion law (1) from a linear dependence.³ This deviation is small ($\psi_p \ll 1$) but the function ψ_p determines the possible relaxation processes in phonon systems of He II.

When $p < p_c$ the deviation $\psi_p > 0$ and the dispersion is anomalous.⁴ At the saturated vapor pressure, the value of the momentum p_c is given by the equality $cp_c/k_B = 10$ K.⁵ With anomalous dispersion, the conservation laws of energy and momentum allow processes that do not conserve the number of phonons. The fastest of these processes is the three-phonon process (3pp),^{6,7} in which one phonon decays into two phonons or two interacting phonons merge into one phonon.

At $p > p_c$, function $\psi(p) < 0$. With this normal dispersion, three-phonon processes are prohibited by the conservation of energy and momentum. In this case the fastest relaxation process for phonons with $p > p_c$ is the four-phonon process (4pp),^{8,9} in which two phonons interact, giving two phonons in the final state.

The scattering rate of three-phonon processes ν_{3pp} is several orders of magnitude greater than that of four-phonon processes ν_{4pp} .⁷⁻⁹ As a result, the phonons in superfluid helium, form two subsystems.

(1) A subsystem of low-energy phonons with $p < p_c$ (l phonons) in which equilibrium occurs relatively quickly.

(2) A subsystem of high-energy phonons with $p > p_c$ (h phonons) in which equilibrium occurs rather slowly.

The presence of two phonon subsystems, with different relaxation times, leads to unique phenomena in the anisotropic phonon systems of He II. Such systems are created by a heater immersed into He II.^{1,2,10-12} The liquid helium has such a low temperature that thermal excitations can be neglected. When a short current pulse, with a duration t_p , is given to the heater, a phonon pulse is formed by the fast three-phonon processes in the liquid. This l -phonon pulse moves in the “superfluid vacuum” of He II, from the heater to the detector with the velocity c .

In momentum space, the phonons of the pulse are mainly located in a narrow cone with a solid angle $\Omega_p \ll 1$,^{13,14} the dimensions of which are defined by the heater power and the pressure of the liquid. The transverse dimensions $2L_\perp$ of such a highly anisotropic system near the heater are about the dimensions of the heater (1 mm \times 1 mm). The longitudinal dimension $L_\parallel = ct_p$ is defined by the current pulse t_p given to the heater. Such phonon pulses in He II are often called phonon sheets,¹⁵ because the inequality $L_\perp \gg L_\parallel$ is usually satisfied.

In the experiments, Ref. 10, a unique phenomenon was observed: when one short current pulse was given to the heater, two pulses, well separated in time, were detected. The first was formed by l -phonons, and the second formed by h -phonons. From the subsequent experiments (see Refs. 11 and 12), it was unambiguously demonstrated that the h -phonon pulse had not been created in the heater but was created by the l -phonon pulse during its motion from the

heater to the detector. The theory of this surprising phenomenon, when a rather cold l -phonon pulse with temperature close to $T_p \approx 1$ K creates high-energy phonons with energy $\varepsilon \geq 10$ K, was given in Refs. 13 and 14.

In Refs. 13 and 14 it was shown that the l -phonon pulse is in equilibrium due to fast 3pp processes. Within this pulse, h -phonons were created by slow 4pp processes with rate ν_{4pp} . The h -phonons have a group velocity $v_h \leq 189$ m/s that is smaller than the velocity of the l -phonon pulse $c = 238$ m/s. The difference in these velocities and the relatively weak relation between h -phonons and l -phonons ($\nu_{3pp} \gg \nu_{4pp}$), leads to the h -phonons leaving the l -phonon pulse through its rear wall and forming the pulse of h -phonons. It arrives at the detector after the l -phonon pulse.

Recently another unique phenomenon in the anisotropic phonon systems of He II was observed.² In the experiments described in Ref. 2, a large increase in the l - and h -phonon signals was observed. This was caused by the interaction of two phonon sheets when they intersected. This interaction occurs during the motion of sheets from the heater to the detector when the angle α between the normals to the centers of the sheets' surfaces, is small. The new formation, created by the intersection of the two sheets in Ref. 2, was called a hot line. Later we shall adhere to this nomenclature.

The increase in the l - and h -phonon signals and the corresponding structure of the hot line depends on the angle α . At one value of α , both l - and h -phonon signals are increased. At a larger value of α , only the l -phonon signal is increased. At an even larger value of α , l - and h -phonon signals remained the same, or even decreased slightly. It was explained in Ref. 2 that the hot line cannot be formed at large angles due to the limited angles involved in 3pp scattering.

The situation can be changed continuously if we increase the pressure of He II. With increasing pressure, the value of p_c monotonically decreases, reaching zero at a pressure of $P_{pr} = 19$ bar.^{5,16,17} At $P_{pr} \geq 19$ bar, the phonon dispersion of He II is normal and only four-phonon processes are allowed. New experiments¹ suggest that there is a need to investigate theoretically the effect of pressure on a single sheet and on two interacting sheets and compare them with these experimental results. The creation of a theory that can describe the unique phenomena observed in Refs. 1 and 2, which are connected with the formation of a hot line, is doubtless of interest. The first results of such a theoretical analysis are given in this paper.

In Sec. II we develop the quasiequilibrium distribution function for anisotropic phonon systems. We derive the relationship between the parameters of the exact distribution function and the approximate, but more physically intuitive, distribution function in which there is a cone of occupied states in momentum space (the step function approximation). In Sec. III we consider the conditions that allow a hot line to form. In Sec. IV we analyze the parameters of the distribution function for the hot line and its relationship to the corresponding parameters for the two sheets that interact. In Sec. V we draw our conclusions.

II. QUASIEQUILIBRIUM DISTRIBUTION FUNCTION OF ANISOTROPIC PHONON SYSTEM

In this section we describe the exact distribution function for the phonons in the sheet and relate it to the intuitive, but

approximate, distribution function introduced earlier. A distribution function gives the occupation of phonon states in angle as well as energy.

The experimental apparatus^{1,2} for investigating the properties of highly anisotropic phonon systems contains a heater and a detector, both immersed in liquid ⁴He at a temperature ~ 0.05 K, where thermal excitations can be neglected. The heater is a metal film deposited on glass heated by a current pulse that injects a pulse of phonons into this pure and isotropic superfluid helium ("the superfluid vacuum"). The evaporated gold film is rough and so we do not expect a critical cone for emission, as results from acoustic theory.¹⁸ However, the phonon emission from a short heating pulse in the gold film, creates a large number of phonons with an average momentum in the direction of the surface normal.

Fast three-phonon processes form an l -phonon pulse from these phonons, which moves in coordinate space from the heater to the detector. Meanwhile in momentum space, l -phonons are formed mainly inside a narrow cone with solid angle $\Omega_p \ll 1$. High-energy phonons (h -phonons) interact with l -phonons relatively weakly, by slow four-phonon processes. The difference in the group velocities of l - and h -phonons results in the h -phonons leaving from the back of the main l -phonon pulse. In this paper we will not consider the contribution of h -phonons to the processes being considered.

The fast three-phonon processes involve small angles. This is justified using an approximate quasiequilibrium function in all previous calculations (see, for example, Refs. 13 and 14), given by

$$n_p = \frac{\eta(\mathbf{ps}/p - \cos \theta_p)}{\exp(\varepsilon/k_B T_p) - 1}, \quad (2)$$

where η is the Heaviside step function, which is equal to zero when the argument is negative, and is equal to unity when the argument is greater than or equal to zero, and \mathbf{s} is the axis of symmetry.

The approximation (2) includes all the necessary parameters of anisotropic systems: temperature T_p , the direction of the axis \mathbf{s} of the anisotropic system, and the value of anisotropy, which is given by angle θ_p , where $\Omega_p = 2\pi(1 - \cos \theta_p)$. It has a simple physical meaning; it is a cone with angle θ_p , cut from an isotropic distribution with temperature T_p . The approximation (2) has allowed the successful solution of a number of problems.^{13,14,19,20}

However, this function (2) cannot be used to solve the problem considered in this paper, namely the interaction of intersecting phonon pulses and the creation of the hot line, observed in Ref. 2. This is because the function (2) does not make the collision integral, for 3pp, equal to zero. For the solution of this problem one should start from the exact quasiequilibrium distribution function, which strictly, and not approximately, makes the integral of three-phonon interactions in the kinetic equation equal to zero, and describes the anisotropy of the phonon system. The exact function is the Bose distribution that includes the drift velocity \mathbf{u} ,

$$n_u = \left[\exp\left(\frac{\varepsilon - \mathbf{pu}}{k_B T}\right) - 1 \right]^{-1}. \quad (3)$$

The function (3) can be written as follows:

$$n_u = \left[\exp\left(\frac{cP}{k_B T_u} \left(1 + \frac{\zeta}{\zeta_u}\right)\right) - 1 \right]^{-1}, \quad (4)$$

where

$$\zeta = 1 - \cos \theta, \quad (5)$$

θ is the angle between the momentum of phonon \mathbf{p} and the drift velocity \mathbf{u} , and

$$\zeta_u = \chi + \psi_p - \chi\zeta, \quad (6)$$

$$\chi = 1 - \frac{u}{c}, \quad (7)$$

and

$$T_u = \frac{T}{\zeta_u}. \quad (8)$$

In a weakly anisotropic case, the parameter χ is close to unity. However for strongly anisotropic phonon systems, which correspond to the experiments in Refs. 1 and 2, $\chi \ll 1$. Then the phonons are mainly in a narrow cone with solid angle $\Omega_p \approx 2\pi\zeta_u$ and its axis is directed along $\mathbf{N} = \mathbf{u}/u$. The function (2) is the step approximation to function (3).

In the case of a strongly anisotropic system, which is not uniform in coordinate space, like the phonon pulses being considered, the function (3) is a local (quasiequilibrium) distribution function since its parameters T and \mathbf{u} depend on coordinates and time. The dependences $T(\mathbf{r}, t)$ and $\mathbf{u}(\mathbf{r}, t)$ can be found from the energy and momentum conservation laws (see Refs. 21 and 22). In Ref. 21 we started from the quasiequilibrium function (2) with $\mathbf{s} = \mathbf{s}(\mathbf{r}, t)$ and $T_p = T_p(\mathbf{r}, t)$. It can be shown²² that the initial system of equations, describing the temporal and spatial evolution of functions $\mathbf{u}(\mathbf{r}, t)$ and $T(\mathbf{r}, t)$, can be rewritten, after the introduction of new variables, in the form of the system of equations for functions $\mathbf{s} = \mathbf{s}(\mathbf{r}, t)$ and $T_p = T_p(\mathbf{r}, t)$, which was solved in Ref. 21. So, the results obtained in Ref. 21 with function (2) can be applied to describe the functions $\mathbf{u}(\mathbf{r}, t)$ and $T(\mathbf{r}, t)$, in Eq. (3). This result will be used in the calculations presented in Sec. III.

Starting from the equality of energies and momenta of anisotropic phonon systems, calculated with a help of distribution functions (2) and (3), we have

$$\int \varepsilon n_p d^3p = \int \varepsilon n_u d^3p, \quad (9)$$

$$\int \mathbf{p} n_p d^3p = \int \mathbf{p} n_u d^3p. \quad (10)$$

It follows from Eq. (10) that axes of anisotropy \mathbf{s} in function (2) and $\mathbf{N} = \mathbf{u}/u$ in function (3) are congruent.

The step approximation (2) is more easy to visualize than the precise function (4); the anisotropic system is just a segment of the isotropic system at T_p . The calculations with the more simple function (2) can often be completed analytically. The resulting analytical expressions, which contain the

parameters $\zeta_p = 1 - \cos \theta_p$ and T_p , enable a simple physical insight to be obtained. Therefore, in later calculations we shall often specify numerical values of the parameters ζ_p and T_p that are connected to the parameters χ and T of the precise function, by the relations (9) and (10).

III. RATE OF INTERACTION OF PHONONS AT THE INTERSECTION OF SHEETS AND THE CONDITIONS FOR HOT LINE CREATION

In this section we consider the 3pp rate and see how it leads to the conditions necessary for the interaction of two phonon sheets and the formation of a hot line. We include the transverse expansion of the sheets as they propagate, as this determines the geometry of the sheets at the line of interaction. We shall see that the sheets, which are planar near their centers, are not planar at their edges. They are curved with a radius of curvature that is approximately equal to the distance from the center of the heater to the point on the sheet.

A. The scattering rate as a function of angle alpha, temperature, and pressure

When the phonon sheet moves from a heater to a bolometer, along the straight line that we call a z axis, it is subjected to transverse expansion along the x axis, which is perpendicular to the z axis (see Refs. 21 and 22). In a symmetrical way, a second sheet moves along the z' axis and expands along the x' axis. The angle between the axes z and z' we call α .

In the region of intersection of the two sheets, phonons from the different sheets start to interact with each other by three-phonon processes. This can be considered as the interaction between two cones, each of which is determined by the two local equilibrium distribution function (3), with different values of the local drift velocities \mathbf{u} and \mathbf{u}' and temperatures T and T' . The symmetry of the problem follows from the initial conditions:^{1,2}

$$|\mathbf{u}| = |\mathbf{u}'| \text{ and } T = T'. \quad (11)$$

The angle $\theta_{\mathbf{u}\mathbf{u}'}$ between vectors \mathbf{u} and \mathbf{u}' is given by

$$\theta_{\mathbf{u}\mathbf{u}'} = \alpha + 2\theta_z, \quad (12)$$

where

$$\theta_z = \arcsin \frac{u_x}{u} \quad (13)$$

is the angle of rotation of the vector \mathbf{u} with respect to the z axis. The angle θ_z increases as the sheet expands (see Ref. 21).

The distribution function, which is the sum of two distribution functions (3), with the velocities \mathbf{u} and \mathbf{u}' makes the collision integral for the three-phonon processes not equal to zero. Therefore three-phonon processes lead to the creation of a new local equilibrium distribution function, which is described in Sec. IV of this paper.

The rate of interaction ν_{3pp} , between two cones with drift velocities \mathbf{u} and \mathbf{u}' , depends on the pressure P_{pr} of the liquid

helium and is a function of the angle $\theta_{uu'}$ between the axes of the two interacting cones and the four scalar parameters that satisfy the equalities (11). It is convenient to take ζ_p and T_p as the scalar parameters, which, as shown in Sec. III, are uniquely defined by the parameters u and T , which determine the distribution function (3). Finally, we take the functional dependencies of ν_{3pp} as

$$\nu_{3pp} = \nu_{3pp}(\theta_{uu'}, T_p, \zeta_p, P_{pr}). \quad (14)$$

The parameter ζ_p is defined by the conditions of the sheet formation near the heater. As pressure increases, the critical angle θ_{3pp} , at which three-phonon processes are still allowed by energy and momentum conservation laws, decreases because the maximum value of the deviation ψ_{\max} from a linear dispersion law (1), decreases. Therefore, with increasing pressure, the parameter ζ_p decreases under otherwise equal conditions. In all calculations in this section we take the equality

$$\zeta_p = \psi_{\max}/2, \quad (15)$$

which is consistent with relation (6) and represents the pressure dependence of ζ_p . It is obvious that equality (15) is a qualitative approximation to the real situation, but it allows us to carry out our calculations in this section without solving the hard problem of the formation of ζ_p near the heater and its pressure and power dependence. Starting from experimental data³ and relation (15), we obtain values of the parameter ζ_p at different pressures that are used in the calculations. At $P_{pr}=0$ bar we have $\zeta_p=0.023$; at $P_{pr}=5$ bar we have $\zeta_p=0.011$; at $P_{pr}=10$ bar we have $\zeta_p=0.0046$; at $P_{pr}=12$ bar we have $\zeta_p=0.003$; at $P_{pr}=18$ bar we have $\zeta_p=0.00079$.

The interaction rate ν_{3pp} of two cones with different values of the parameters contained on the right side of Eq. (14) have been calculated using the results of Ref. 7 and Ref. 23. In Figs. 1(a) and 1(b) the graphs show the results obtained from Ref. 23. In this figure we see that the dependence of ν_{3pp} on angle $\theta_{uu'}$, has a maximum at a nonzero angle. The physical reasons for this maximum are discussed in detail in Ref. 23. Here we only note that the maximum corresponds to the optimum angle that satisfies energy and momentum conservation for three-phonon processes. From Fig. 1(b) one can see that the optimum angle (as well as the critical angle for three-phonon processes θ_{3pp}) decreases with increasing pressure. The value ν_{3pp} decreases with increasing pressure due to changes in the liquid helium parameters. According to Fig. 1(a), the optimum angle and the rate ν_{3pp} also decrease with decreasing temperature. The physical reasons for these dependencies are discussed in detail in Ref. 23.

Parameters θ_z and T_p from the right side of equality (14) are functions of time and the transverse coordinate x :

$$\theta_z = \theta_z(x, t) \text{ and } T_p = T_p(x, t), \quad (16)$$

with initial conditions

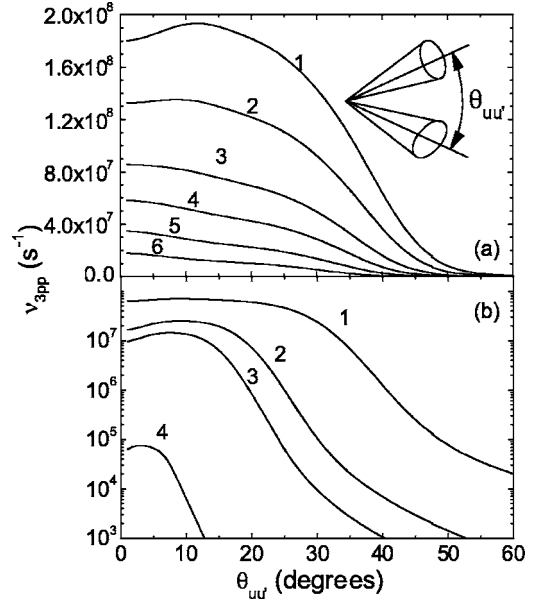


FIG. 1. The scattering rate for 3pp, ν_{3pp} , is shown as a function of angle, $\theta_{uu'}$, between the two cone axes. In (a) curves 1 to 6 are for temperatures T_p 1, 0.9, 0.8, 0.7, 0.6, and 0.5 K, respectively, at 0 bar. In (b) curves 1 to 4 are for pressures 5, 10, 12, and 18 bar, respectively, at $T_p=1$ K. The value of ζ_p is given by Eq. (15) in all cases.

$$\theta_z(x, t=0) = 0 \text{ and } T_p(x, t=0) = T_p(0)\eta(L_{\perp} - |x|); \quad (17)$$

here $T_p(0)$ is constant for a given ζ_p . These functional dependencies have been derived in Ref. 21 and we use them in the calculations given here.

B. The transverse expansion

The analysis of the transverse expansion of the phonon sheet²¹ shows that there is a rarefaction wave, in the transverse direction, which moves during the time interval

$$0 \leq t \leq L_{\perp}/c_{\theta}, \quad (18)$$

in the direction toward the center of the sheet (the point with $x=0$), with velocity

$$c_{\theta} = c\sqrt{\zeta_p/2}. \quad (19)$$

Also, the sheet expands along the x axis with the dependences $T_p(x, t)$ and $\theta_z(x, t)$, which are described in Ref. 21 by Eqs. (55) and (56) during the time interval (18). At the time

$$t_r = L_{\perp}/c_{\theta}, \quad (20)$$

the rarefaction wave reaches the point at $x=0$. After this time a reflected wave appears, which propagates from the point $x=0$ to the periphery of the sheet. At $t > t_r$ the reflected wave exists in the region

$$0 < x < x_r, \quad (21)$$

where x_r is the point of a weak break in the wave. In the interval (21), the dependences $T_p(x, t)$ and $\theta_z(x, t)$ are described in Ref. 21 by Eqs. (60)–(63), and the time depen-

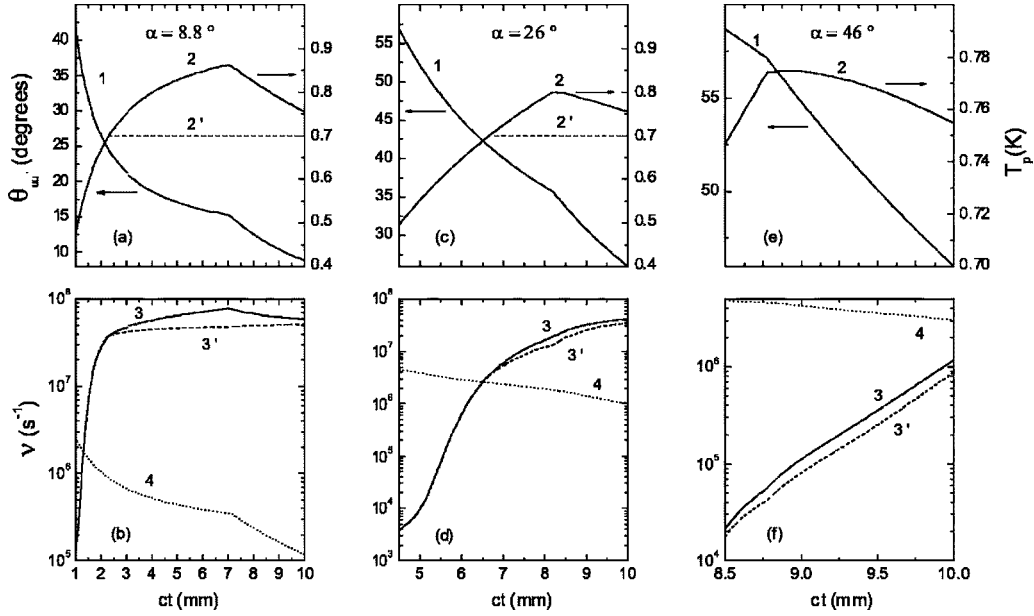


FIG. 2. In the upper frames are the dependences of the angle $\theta_{uu'}$ between the two cone axes \mathbf{u} and \mathbf{u}' (solid curves 1), the temperature T_p of each pulse (solid curves 2) as functions of distance propagated, ct . In the lower frames are shown the three-phonon process rates ν_{3pp} at the saturated vapor pressure, for the interaction between the two phonon cones with angle $\theta_{uu'}$ between their axes (solid curves 3) as functions of the distance propagated, ct . Results for three angles α between the heaters are shown: $\alpha=8.8^\circ$ (Fig. 2(a) and Fig. 2(b)), $\alpha=26^\circ$ (Fig. 2(c) and Fig. 2(d)), $\alpha=46^\circ$ (Fig. 2(e) and Fig. 2(f)). The dashed curves 2' show a maximum temperature for the phonon pulses of 0.7 K, and the dashed curves 3' show the corresponding three-phonon processes rate ν_{3pp} . The dependences of the inverse of the time to cross the region of overlap of the two phonon pulses, $\nu_{cross} = t_{cross}^{-1}$, is shown as a function of the distance propagated, ct , dotted curves 4. In all cases the pressure is the saturated vapor pressure, the duration of the phonon pulses is $t_p = 100$ ns, the transverse size of the pulses is $L_\perp = 0.5$ mm, the initial temperature of the pulses is $T_p = 1$ K, the parameter of anisotropy is $\zeta_p = 0.023$, and the distance between the centers of the heaters and the center of the bolometer is $R = 10$ mm.

dence of the coordinate of the weak break at x_r is given in Ref. 21 by Eq. (65). At the point $x = x_r$, the solutions (60)–(63) of Ref. 21, that includes the reflected wave, should be joined to solutions (55) and (56) in Ref. 21 for the rarefaction wave, to make the function continuous. The derivatives are discontinuous, which is why the point x_r is called a point of weak break. This point is clearly seen as a discontinuity in the slope of the curves in Figs. 2 and 3, at 0 and 5 bar.

C. Results

The variable x , contained in function (16), should be equal to coordinate x_{cross} , the point of intersection of the sheets, which, at time t , is given by

$$x_{cross} = (R - ct) \tan \frac{\alpha}{2}, \quad (22)$$

where R is the distance from the heater to the bolometer. In the experiment,² $R = 10$ mm. In a later experiment,¹ $R = 13$ mm, but we shall use $R = 10$ mm in all numerical calculations, as this causes no qualitative change.

The substitution of (22) into functions (16) and (17), gives the time dependence

$$\theta_z(t) = \theta_z \left(x = (R - ct) \tan \frac{\alpha}{2}; t \right) \quad (23)$$

and

$$T_p(t) = T_p \left(x = (R - ct) \tan \frac{\alpha}{2}; t \right). \quad (24)$$

Substituting Eqs. (23) and (24), into Eq. (14), gives the time dependence of the 3pp rate,

$$\nu_{3pp} = \nu_{3pp}[\alpha + 2\theta_z(t), T_p(t), \zeta_p, P_{pr}]. \quad (25)$$

In Figs. 2 and 3, curves 1 show the dependence (12), where θ_z is defined by (23), curves 2 show the dependence (24), and curves 3 show the dependences (25). The curves are calculated for different values of angle α or pressure P_{pr} . In all cases, the initial temperature of the sheets $T_p(0)$ was taken equal to 1 K.

At small t , when the sheets are near the heaters, they intersect in the outer regions of the sheets formed by the transverse expansion. The temperature T_p is low in these outer areas, and angle θ_z is high. As a result, we see from Fig. 1 that the 3pp rates, ν_{3pp} , are small (see curves 3 in Figs 2 and 3). As the sheets move from the heater to the bolometer in the region of intersection of the sheets, the temperature T_p increases and the angle θ_z decreases. As a result, the rate ν_{3pp} increases.

In Figs. 2 and 3, discontinuities of slope on curves 1 and 2, at $P_{pr} = 0$ and 5 bar, correspond to the time $t_{w.b.}$, when the point of intersection of the sheets coincides with the point x_r of the weak break. In this case, the temperature at the point of intersection of the sheets never reaches its initial value

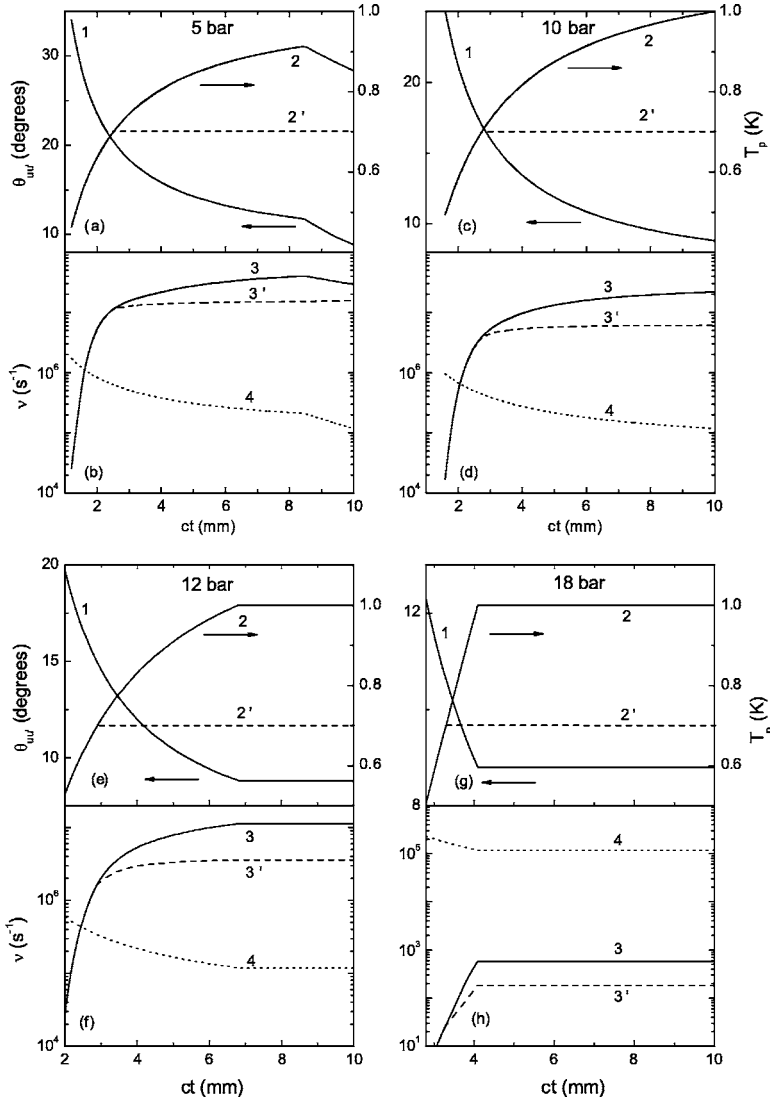


FIG. 3. Curves similar to Fig. 2 are shown for four representative pressures. In the upper frames are the dependencies of the angle $\theta_{\mathbf{u}\mathbf{u}'}$ between the two cone axes \mathbf{u} and \mathbf{u}' (solid curves 1), the temperature T_p of each pulse (solid curves 2) as functions of distance propagated, ct . In the lower frames are shown the three-phonon process rates ν_{3pp} at different pressures, for the interaction between the two phonon cones with angle $\theta_{\mathbf{u}\mathbf{u}'}$ between their axes (solid curves 3) as functions of the distance propagated, ct . Results for four pressures are shown, $P_{pr}=5$ bar (Fig. 3(a) and Fig. 3(b)), $P_{pr}=10$ bar (Fig. 3(c) and Fig. 3(d)), $P_{pr}=12$ bar (Fig. 3(e) and Fig. 3(f)), and $P_{pr}=18$ bar (Fig. 3(g) and Fig. 3(h)). The dashed curves 2' show a maximum temperatures for the phonon pulses of 0.7 K, and the dashed curves 3' show the corresponding three-phonon processes rate ν_{3pp} . The dependencies of the inverse of the time to cross the region of overlap of the two phonon pulses, $\nu_{cross}=t_{cross}^{-1}$, is shown as functions of the distance propagated, ct , dotted curves 4. In all cases the angle between heaters $\alpha=8.8^\circ$, the duration of the phonon pulses is $t_p=100$ ns, the transverse size of pulses is $L_\perp=0.5$ nm, the initial temperature of the pulses is $T_p=1$ K, the parameter of anisotropy is given by Eq. (15) and the distance between the centers of the heaters and the center of the bolometer is $R=10$ mm.

$T_p(0)=1$ K. This can be explained in the following way: at small $\alpha=8.8^\circ$, the velocity (19) of the rarefaction wave moving toward the center of the sheet, is greater than the velocity of relative motion of the sheets. Then the rate of cooling of the sheets is faster than the energy gain by the hot line, from the sheets. At the larger values of the angles $\alpha=26^\circ$ and 46° , the initial distance between the ends of the sheets is so large that the temperature, in the region of intersection (see curves 2 in Fig 2), never reaches the temperature in the center of the sheets that is at most equal to the initial temperature $T_p(0)=1$ K.

At $t > t_{w,b}$ (see curves 3 in Fig. 2 and Fig. 3(b)) the change of ν_{3pp} with time, is determined by two opposing factors.

(1) An increase in ν_{3pp} due to the change in angle $\theta_{\mathbf{u}\mathbf{u}'}$ between the cones. At $ct=10$ mm the intersection point of the sheets is at their centers, where $\theta_z(x=0)=0$. Thus the angle $\theta_{\mathbf{u}\mathbf{u}'}$ reaches the minimum value that is equal to α .

(2) A decrease in ν_{3pp} due to temperature T_p decreasing at $t > t_{w,b}$.

At a small value of the angle $\alpha=8.8^\circ$ and at pressures $P_{pr}=0$ bar and 5 bar, the second factor dominates and ν_{3pp} decreases with time when $t > t_{w,b}$ (see curve 3, Figs. 2(b) and

3(b)). At the larger angles $\alpha=26^\circ$ and 46° , the first factor dominates and ν_{3pp} increases with time when $t > t_{w,b}$, and $\theta_{\mathbf{u}\mathbf{u}'}$ decreases (see a curve 3 in Figs. 2(d) and 2(f)).

The situation changes at high pressures. As ζ_p decreases, the velocity relative to c (19), decreases. The temperature of the sheet, where the sheets intersect, has its initial value $T_p(0)=1$ K for some of the distance (see a curve 2 in Figs. 3(c), 3(e), and 3(g)). Then the angle $\theta_{\mathbf{u}\mathbf{u}'}=\alpha$ and the rate ν_{3pp} does not depend on time.

D. Conditions for the formation of a hot line

Whether a hot line forms or not depends on the relative sizes of the rate ν_{3pp} and $\nu_{cross}=t_{cross}^{-1}$, where t_{cross} is the time to cross the region where the two sheets overlap, i.e., the length of the large diagonal of the rhombus of the region of overlap $d_{beg}=L_\parallel/\sin(\alpha/2+\theta_z)$ divided by the velocity of the sheets' relative motion. As a result we obtain

$$\nu_{cross}=t_p^{-1}2\sin^2\left(\frac{\alpha}{2}+\theta_z\right). \quad (26)$$

According to (12) and (26), the time dependence of ν_{cross} is completely defined by the function $\theta_{\mathbf{u}\mathbf{u}'}(t)$, which is shown in Figs. 2 and 3 by curves 1, for a variety of conditions. The dependence $\nu_{cross}(t)$ when $t_p=100$ ns ns at different pressures and angles α , is given by the dotted lines 4 in Figs. 2 and 3. The explanation of these dependencies is the same as we have given above for $\theta_z(t)$.

A hot line is formed if

$$\nu_{3pp} > \nu_{cross}. \quad (27)$$

If the inequality (27) is valid, phonons have time to interact in the region of intersection of the sheets and to create a hot line. If the inequality

$$\nu_{3pp} < \nu_{cross} \quad (28)$$

applies, then phonons do not have time to interact in the region of intersection, so the sheets pass through each other and no hot line is formed.

The inequalities (27) and (28) and the curves 3 and 4 in Figs. 2 and 3 tell us when and at what distance from the heater a hot line starts to form and when the formation of a hot line is not possible. So when $\alpha=8.8^\circ$ at $P_{pr}=0$ bar, the hot line starts to form at distance ~ 1.3 mm from the heater; at $P_{pr}=5$ bar, the distance is ~ 1.6 mm; at $P_{pr}=10$ bar, ~ 2.1 mm; at $P_{pr}=12$ bar, ~ 2.5 mm; and for the pressure $P_{pr}=18$ bar the inequality (28) is always true and a hot line is not formed. These results are in agreement with the experimental data of Ref. 1. When $\alpha=26^\circ$ and $P_{pr}=0$ bar, the hot line forms at a distance ~ 6.5 mm from the heater, and when $\alpha=46^\circ$ according to (28) and in Fig. 2(f) a hot line does not form. These results are in the agreement with experimental data of Ref. 2.

In concluding this section, we note that the calculations made here and the graphs in Figs. 2 and 3, are only strictly correct for sufficiently cold sheets, when we can neglect the creation of h -phonons. However, it is easy to estimate how the rate ν_{3pp} and the results obtained above will change if we take into account the creation of h -phonons. As the created h -phonons leave the sheet through the rear wall of the sheet, the hot region of the sheet will cool to a temperature of about 0.7 K at $P_{pr}=0$,^{13,14} after which, the creation of h -phonons will finish. Such regions of uniform temperature were observed in experiments, Ref. 15. The formation of such regions in our calculations can be taken into account if in Figs. 2 and 3 curves 2 at $T>0.7$ K are replaced by horizontal dashed lines, labeled 2', which limits the temperatures rise to 0.7 K. The results of calculations, obtained with this temperatures limit, give rates ν_{3pp} that are shown by the dashed lines, labeled 3', in Figs. 2 and 3. These new values of the rates ν_{3pp} do not affect the arguments made above about the possibility of a hot line forming under the conditions considered above.

IV. LOCAL EQUILIBRIUM DISTRIBUTION FUNCTION OF A HOT LINE

In this section we derive the distribution function for the hot line in terms of the parameters describing the sheets.

A. General description of the distribution function

When two identical pulses intersect, in the region of intersection the initial distribution function n_{in} is equal to the sum of the two distribution functions from the two pulses (see Eq. (3)), hence

$$n_{in} = n(\mathbf{p}, \mathbf{u}, T) + n(\mathbf{p}, \mathbf{u}', T), \quad (29)$$

which only differ from each other in their directions of the drift velocities \mathbf{u} and \mathbf{u}' ; the values of their moduli are equal. According to Eq. (3) the initial state (29) is completely defined by two unit vectors and two scalar parameters,

$$\mathbf{N} = \mathbf{u}/u; \quad \mathbf{N}' = \mathbf{u}'/u; \quad \chi; \quad T. \quad (30)$$

The initial distribution function (29) does not make the integral of the three-phonon collisions equal to zero. As a result, 3pp scattering in a time ν_{3pp}^{-1} causes a new local equilibrium distribution function n_{hl} with parameters \mathbf{u}_{hl} and T_{hl} (see Eq. (3)) that describes the hot line. We consider that the time to cross the common volume ν_{cross}^{-1} is greater than ν_{3pp}^{-1} . The new local distribution function is completely defined by the parameters

$$\mathbf{N}_{hl} = \mathbf{u}_{hl}/u_{hl}; \quad \chi_{hl}; \quad T_{hl}. \quad (31)$$

We wish to derive the parameters (31) when the parameters (30) are given. The relation between parameters (30) and (31) can be obtained from energy conservation,

$$2E = E_{hl} \quad (32)$$

and momentum conservation

$$\mathbf{P} + \mathbf{P}' = \mathbf{P}_{hl}, \quad (33)$$

where E and E_{hl} are the energy densities of the phonons in the initial and final states, respectively, and \mathbf{P} , \mathbf{P}' , and \mathbf{P}_{hl} are the densities of the phonon momenta in the initial and final states, respectively. The equalities (11) give

$$P = P'. \quad (34)$$

The axes of anisotropy of the initial and final states are directed along their momenta so that

$$\mathbf{N} = \frac{\mathbf{P}}{P}; \quad \mathbf{N}' = \frac{\mathbf{P}'}{P'}; \quad \mathbf{N}_{hl} = \frac{\mathbf{P}_{hl}}{P_{hl}}. \quad (35)$$

From relations (33) and (34) it follows that the axis of anisotropy \mathbf{N}_{hl} is directed along the bisector of the angle $\theta_{\mathbf{u}\mathbf{u}'}$ between vectors \mathbf{N} and \mathbf{N}' (see the inset in Fig. 4).

From (33) and (35) we have

$$2P \cos \frac{\theta_{\mathbf{u}\mathbf{u}'}}{2} = P_{hl}. \quad (36)$$

The equations (32) and (36) give the relationship between parameters χ , T and parameters χ_{hl} , T_{hl} . However, for calculations, the system (32) and (36) are inconvenient, as they contain expressions for densities of energy and momentum that only differ from each other by the small value of average $\langle \psi_p \rangle$ and by the parameter of anisotropy average $\langle \zeta \rangle$, which for this strongly anisotropic initial phonon system, is also small. Therefore it is convenient, using Eq. (32), to convert

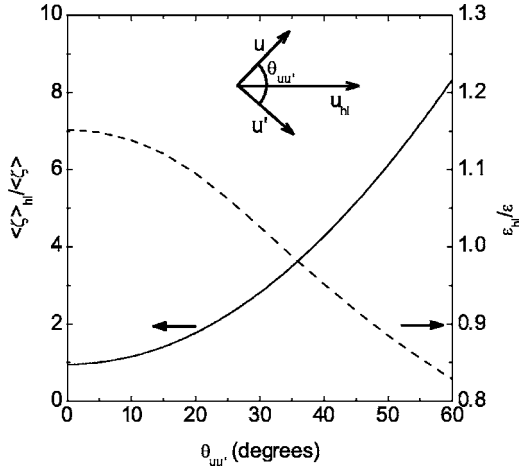


FIG. 4. The dependencies of the ratio $\langle \zeta \rangle_{hl} / \langle \zeta \rangle$ of energy averages (solid curve) and of the ratio $\bar{\varepsilon}_{hl} / \bar{\varepsilon}$ of usual averages (dashed curve) as functions of the angle $\theta_{\mathbf{u}\mathbf{u}'}$ between \mathbf{u} and \mathbf{u}' . We see that $\langle \zeta \rangle_{hl}$ increases with angle $\theta_{\mathbf{u}\mathbf{u}'}$, and the average energy of the phonons in the hot line decreases with angle. The inset shows the vectors \mathbf{u} and \mathbf{u}' of the two pulses that interact, and \mathbf{u}_{hl} of the hot line. The initial values of parameters of distribution function (4) were equal to $T=0.025$ K and $\chi=0.020$ and corresponded to $\langle \zeta \rangle = 0.018$ and $\bar{\varepsilon} = 1.21$ K.

Eq. (36) so that it contains the difference $E - cP$ that is proportional to the perturbations $\langle \psi_p \rangle$ and $\langle \zeta \rangle$. As a result, we have

$$\frac{E - cP}{E} + \frac{cP}{E} \zeta_{\mathbf{u}\mathbf{u}'} = \frac{E_{hl} - cP_{hl}}{E_{hl}}, \quad (37)$$

where

$$\zeta_{\mathbf{u}\mathbf{u}'} = 1 - \cos \frac{\theta_{\mathbf{u}\mathbf{u}'}}{2}. \quad (38)$$

Substitution of the explicit expressions for E and P into Eqs. (32) and (37), gives the following combined equations:

$$\begin{aligned} 2(1 + \langle \psi_p \rangle) \int_0^{p_c} \int_0^2 n(p, \zeta) p^3 dp d\zeta \\ = (1 + \langle \psi_p \rangle_{hl}) \int_0^{p_c} \int_0^2 n_{hl}(p, \zeta) p^3 dp d\zeta, \end{aligned} \quad (39)$$

$$\frac{\langle \psi_p \rangle + \langle \zeta \rangle (1 - \zeta_{\mathbf{u}\mathbf{u}'}) + \zeta_{\mathbf{u}\mathbf{u}'}}{1 + \langle \psi_p \rangle} = \frac{\langle \psi_p \rangle_{hl} + \langle \zeta \rangle_{hl}}{1 + \langle \psi_p \rangle_{hl}}, \quad (40)$$

where the energy averages, contained in the equations (39) and (40), are determined by the equality

$$\langle F \rangle = \frac{\int_0^2 \int_0^{p_c} F(p, \zeta) n(p, \zeta) p^3 dp d\zeta}{\int_0^2 \int_0^{p_c} n(p, \zeta) p^3 dp d\zeta}. \quad (41)$$

We write the same subscript in the left part of equality (41), as in the distribution function $n(p, \zeta)$, which occurs in the integrand on the right side of equality (41).

The combined equations (39) and (40) are precise and allow us to find the values of parameters χ_{hl} , T_{hl} if we know the values of parameters χ , T . However, it is sufficiently precise for our calculations to use the simpler but approximate combined equations found by taking into account that

$$\langle \psi_p \rangle \ll 1; \quad \langle \psi_p \rangle_{hl} \ll 1; \quad \langle \zeta \rangle \ll 1. \quad (42)$$

The inequalities (42) allow us to ignore the inessential terms $\langle \psi_p \rangle$ and $\langle \psi_p \rangle_{hl}$ in the equation (39), and in the equation (40) we restrict ourselves to the linear approximation in the small parameters (42). As a result, we have

$$2 \int_0^{p_c} \int_0^2 n(p, \zeta) p^3 dp d\zeta = \int_0^{p_c} \int_0^2 n_{hl}(p, \zeta) p^3 dp d\zeta, \quad (43)$$

$$(\langle \psi_p \rangle + \langle \zeta \rangle)(1 - \zeta_{\mathbf{u}\mathbf{u}'}) + \zeta_{\mathbf{u}\mathbf{u}'} = \langle \psi_p \rangle_{hl} + \langle \zeta \rangle_{hl} [1 - \langle \psi_p \rangle_{hl}]. \quad (44)$$

The combined equations (43) and (44) were the starting point of all numerical calculations in this section. The deviation of the dispersion law (1) from linearity was approximated with the function

$$\psi_p = 4\psi_{\max} \left(\frac{p}{p_c} \right)^2 \left[1 - \left(\frac{p}{p_c} \right)^2 \right], \quad (45)$$

where

$$\psi_{\max} = \psi(p = p_c \sqrt{2}) \quad (46)$$

is a maximum value of function (45). The approximation (45) reflects all the main properties of the dependence $\psi_p = \psi(p)$ that were observed in experiments³ and contains two parameters, the numerical values of which were obtained from experimental data;³ at the saturated vapor pressure $\psi_{\max} = 0.046$ and $cp_c/k_B = 10$ K.

The maximum value of angle $\theta_{\mathbf{u}\mathbf{u}'} = \pi$ is reached when the maximum value of parameter $\zeta_{\mathbf{u}\mathbf{u}'} = 1$. The substitution of this value to the equation (44) gives the maximum value of the parameter of anisotropy $\langle \zeta \rangle_{hl} = 1$ at which, according to (41), the function n_{hl} does not depend on ζ , i.e., the phonon system is completely isotropic. Thus, corresponding with energy conservation (43), the temperature T_{hl} appears minimal. With decreasing $\zeta_{\mathbf{u}\mathbf{u}'}$, $\langle \zeta \rangle_{hl}$ decreases according to Eq. (44), and the temperature T_{hl} corresponding with equality (43) increases.

As we can see from conservation laws (9) and (10) the equalities (43) and (44) are satisfied, not only with the exact function n_u , but with the step approximation n_p , which allows us to make all necessary integrations and to obtain the

analytical expressions that contain parameters ζ_p and T_p , which have a simple physical sense. Substituting (2) into Eqs. (43) and (44) we have a system of two equations with two variables $\zeta_{p,hl}$ and $T_{p,hl}$, and the parameters ζ_p , T_p , and $\zeta_{uu'}$ are considered, given

$$2\zeta_p T_p^4 = \zeta_{p,hl} T_{p,hl}^4, \quad (47)$$

$$\left(\varphi(T_p) + \frac{\zeta_p}{2} \right) (1 - \zeta_{uu'}) + \zeta_{uu'} = \varphi(T_{p,hl}) + \frac{\zeta_{p,hl}}{2} [1 - \varphi(T_{p,hl})], \quad (48)$$

where according to Eqs. (45) and (41),

$$\varphi(T) = 80 \frac{\zeta(6)}{\zeta(4)} \psi_{\max} \left(\frac{k_B T}{c p_c} \right)^2 \left\{ 1 - 42 \frac{\zeta(8)}{\zeta(6)} \left(\frac{k_B T}{c p_c} \right)^2 \right\}, \quad (49)$$

where $\zeta(4)=1.082$, $\zeta(6)=1.017$, $\zeta(8)=1.004$ are the values of the Riemann zeta function.

B. Evaluation of the distribution function

The combined equations (47) and (48) can be solved analytically. Here we restrict ourselves to getting results that follow from (47) and (48) after simple evaluations.

At given values of ζ_p and T_p , we find values $\zeta_{p,hl}$ and $\zeta_{uu'}$ at which the final temperature $T_{p,hl}$ is equal to the initial temperature T_p . In this case from the equations (47) and (48) we get the following:

$$\text{if } T_{p,hl} = T_p \text{ then } \zeta_{p,hl} = 2\zeta_p \text{ and } \zeta_{uu'} = \frac{\zeta_p}{2}. \quad (50)$$

From the equations (47), (48), and (50) it follows that the inequalities written below must be satisfied:

$$\text{if } \zeta_{uu'} > \frac{\zeta_p}{2} \text{ then } T_{p,hl} < T_p; \quad (51)$$

$$\text{if } \zeta_{uu'} < \frac{\zeta_p}{2} \text{ then } T_{p,hl} > T_p. \quad (52)$$

At given ζ_p and T_p we find values $T_{p,hl}$ and $\zeta_{uu'}$ at which the parameters of the anisotropy, in the initial and final states, are equal. In this case from the equations (47) and (48) follows:

$$\text{if } \zeta_{p,hl} = \zeta_p \text{ then } T_{p,hl} = 2^{1/4} T_p \text{ and } \zeta_{uu'} = \varphi(2^{1/4} T_p) - \varphi(T_p). \quad (53)$$

From equality (53), when $T_p=0.7$ K, we have $T_{p,hl}=0.83$ K and $\theta_{uu'} \approx 9.7^\circ$.

From the equations (47), (48), and (53) it follows that the following inequalities are satisfied:

$$\text{if } \zeta_{uu'} < \varphi(2^{1/4} T_p) - \varphi(T_p) \text{ then } \zeta_{p,hl} < \zeta_p. \quad (54)$$

Thus, the interaction of two similar anisotropic phonon systems leads to a decrease in the occupied solid angle $\Omega_{p,hl}$ in momentum space for the hot line. Meanwhile the solution of the system (47) and (48) gives us only the qualitative answer. The precise solution of the problem we can obtain by

numerical solving of the system of equations (43) and (44) with the distribution function (4). Figure 4 represents the results of such a solution, where the dependencies of the ratio $\langle \zeta \rangle_{hl} / \langle \zeta \rangle$ of energy averages (solid curve) and of the ratio $\bar{\varepsilon}_{hl} / \bar{\varepsilon}$ of usual averages ($\bar{\varepsilon} = \int \varepsilon n_u d^3 p / \int n_u d^3 p$) (dashed curve) are shown as functions of the angle $\theta_{uu'}$ between \mathbf{u} and \mathbf{u}' . The initial values of parameters of distribution function (4) were equal to $T=0.025$ K and $\chi=0.020$ and corresponded to $\langle \zeta \rangle=0.018$ and $\bar{\varepsilon}=1.21$ K. In accordance with (9) and (10) to the above mentioned, initial values of χ and T correspond to the values $\zeta_p=0.023$ and $T_p=0.7$, which are typical for interacting pulses, at the saturated vapor pressure, because the pulses cool quickly from a higher initial temperature to about 0.7 K, due to the creation of h phonons (see Refs. 13 and 14).

The analysis of approximate equations (47) and (48) gives us the possibility to understand the physical reasons for the general behavior of the dependencies shown in Fig 4. For example, from this analysis we understand why $\langle \zeta \rangle_{hl}$ of the hot line increases with angle $\theta_{uu'}$, and the average energy of the phonons in the hot line decreases with angle.

In concluding this section we note that in the region of the hot line the following situation is possible: the initial distribution function is equal to the sum of three terms, two of which are the distribution functions of the sheets, and the third is the distribution function of the hot line formed by previous interactions. Such an initial distribution function does not make the integral of the three-phonon collisions equal to zero and in time ν_{3pp}^{-1} gives the new local equilibrium function of the hot line with a new temperature and new drift velocity. The parameters of this new local equilibrium function for the hot line can be obtained using the method developed in this section.

V. CONCLUSION

The results of this paper allow us to understand the physical reasons and mechanisms for the formation of a hot line in liquid helium when two phonon sheets collide, and also to explain a number of experimental results, Refs. 1 and 2.

During the motion of a single phonon sheet from the heater to the detector, there is a transverse expansion of the area of the sheet from its initial dimensions of the heater. As a result of this expansion, only a small fraction of the pulse energy intersects the bolometer, as its dimensions are similar to those of the heater.

Two identical phonon sheets can be made to intersect before they reach the detector. There are only two essentially different situations that are possible.

(1) If the time for the phonon pulses to cross the volume of overlap of the two sheets ν_{cross}^{-1} is less than the time for phonon scattering ν_{3pp}^{-1} , then the phonons from the two pulses have no time to interact. In this case the hot line does not form because the pulses pass through each other without interaction. The evolution in time and space of each pulse is independent of the other. In Sec. IV it is shown that this situation is realized at large values of the angle α between the heaters (see Fig. 2(f)), or at sufficiently high pressures (see Fig. 3(h)). In this case the amplitude of the signal from

the bolometer, from two simultaneously injected pulses, should be equal to the sum of the amplitudes of the signals from separate pulses at different times. Such a result was obtained in experiments, Refs. 1 and 2, when the angle between heaters was 46° or when pressure was an equal to 18 bar. The calculations of actual numerical values (see Figs. 2(f) and 3(h)) are in the agreement with the results of experiments, Refs. 1 and 2.

(2) If the time for the phonon pulses to cross the volume of overlap ν_{cross}^{-1} of the two sheets is greater than the time of phonon relaxation ν_{3pp}^{-1} (see Figs. 2(b), 2(d), 3(b), 3(d), and 3(f)), then phonons from the two pulses have enough time to interact with each other and to create a hot line in the region where the pulses intersect. According to Sec. V, such a hot line can be described by a local equilibrium distribution function n_{hl} in which the drift velocity u is close to c and is directed along the axis of symmetry (see the inset in Fig. 4). This axis of symmetry is perpendicular to the plane of the bolometer. In this case some of the energy of the expanding pulses accumulates in the hot line, travels along the axis of symmetry and intercepts the bolometer. As a result the amplitude of the l -phonon signal always appears greater than the sum of the signals from pulses that move independently to the bolometer. The observation of this phenomenon in Refs. 1 and 2 stimulated the creation of the theory presented in this paper.

According to inequalities (51) and (52), the structure of the phonon energy, concentrated in the region of the hot line, depends on the angle between the interacting pulses. When the value of the angle $\theta_{uu'}$ is rather small (see inequality (52)) there is a rise in the temperature of the hot line, which should lead to the increase in the number of h phonons created by the hot line. Thus, there will be an increase in the h -phonon signal as well as in the l -phonon signal. Such a phenomenon was observed in Refs. 1 and 2 at small values of the angle α between the heaters. The phonon signal is in the agreement with estimations based on the inequality (52).

When the value of the angle $\theta_{uu'}$ is larger (see the inequality (51)) but the sheets still interact, there is a decrease in the temperature of the hot line. In this case it should be

called a cold line. Nevertheless in this region there is an increase in the phonon energy density, because in the final state, the phonons occupy a phase volume that is twice that of the initial state ($\zeta_{p,hl} > 2\zeta_p$ (see Eq. (50))). So even in this case there is an increase in the l -phonon signal that is greater than the sum of signals of separate pulses. The situation for h -phonons is quite different: their creation is more dependent on the temperature of l -phonons than on the volume of phase space occupied by the l -phonons (see Refs. 13, 14, and 20). A decrease in the temperature of the cold line should cause the h -phonon signal to be less than the sum of amplitudes of h -phonon signals from separate pulses. Such a result was obtained in experiments Ref. 2 when the angle between heaters was equal to 26 deg. This numerical value is in the agreement with estimations based on inequality (51).

In concluding this paper, we note that we correctly understand the physical reasons and mechanisms of the hot line formation, and it enables us to explain a number of experimental results, Refs. 1 and 2. Meanwhile there are results in Refs. 1 and 2, which are waiting for a theoretical explanation. It is necessary to note that among them is the unusual nonmonotonic dependence of the l -phonon signal on pressure, which is observed at all powers (see Ref. 1). Also, in some cases there is a nonmonotonic dependence of l -phonon signal amplitude on the power applied to the heater (see Ref. 2). Moreover, there are new experimental results, as yet unpublished, on the dependence of the l -phonon signal amplitude on angle α between heaters. These phenomena are waiting a theoretical analysis.

These and the other unique phenomena that have been observed, is certainly stimulating further development of the theory of anisotropic phonon systems of superfluid helium. On the other hand, we hope that the theory suggested in this paper will stimulate further experimental research in this astonishing area of macroscopic quantum physics.

ACKNOWLEDGMENTS

We express our gratitude to EPSRC of the UK (Grant No. EP/C 523199/1), and to GFFI of Ukraine (Grant No. N02.07/000372) for support for this work.

¹D. H. S. Smith, R. V. Vovk, C. D. H. Williams, and A. F. G. Wyatt, preceding paper, Phys. Rev. B **72**, 054506 (2005).

²R. V. Vovk, C. D. H. Williams, and A. F. G. Wyatt, Phys. Rev. Lett. **91**, 235302 (2003).

³W. G. Stirling, in *75th Jubilee Conference on Liquid Helium-4*, edited by J. G. M. Armitage (World Scientific, Singapore, 1983), p. 109; and private communication.

⁴H. J. Maris and W. E. Massey, Phys. Rev. Lett. **25**, 220 (1970).

⁵R. C. Dynes and V. Narayanamurti, Phys. Rev. Lett. **33**, 1195 (1974).

⁶S. Havlin and M. Luban, Phys. Lett. **42A**, 133 (1972).

⁷M. A. H. Tucker, A. F. G. Wyatt, I. N. Adamenko, A. V. Zhukov, and K. E. Nemchenko, Low Temp. Phys. **25**, 488 (1999) [Fiz. Nizk. Temp. **25**, 657 (1999) in Russian].

⁸M. A. H. Tucker and A. F. G. Wyatt, J. Phys.: Condens. Matter **4**,

7745 (1992).

⁹I. N. Adamenko, K. E. Nemchenko, A. V. Zhukov, M. A. H. Tucker, and A. F. G. Wyatt, Physica B **284–288**, 31 (2000).

¹⁰A. F. G. Wyatt, N. A. Lockerbie, and R. A. Sherlock, J. Phys.: Condens. Matter **1**, 3507 (1989).

¹¹M. A. H. Tucker and A. F. G. Wyatt, J. Phys.: Condens. Matter **6**, 2813 (1994).

¹²M. A. H. Tucker and A. F. G. Wyatt, J. Low Temp. Phys. **113**, 621 (1998).

¹³I. N. Adamenko, K. E. Nemchenko, A. V. Zhukov, M. A. H. Tucker, and A. F. G. Wyatt, Phys. Rev. Lett. **82**, 1482 (1999).

¹⁴A. F. G. Wyatt, M. A. H. Tucker, I. N. Adamenko, K. E. Nemchenko, and A. V. Zhukov, Phys. Rev. B **62**, 9402 (2000).

¹⁵R. V. Vovk, C. D. H. Williams, and A. F. G. Wyatt, Phys. Rev. B **68**, 134508 (2003).

- ¹⁶J. Jäckle and K. W. Kerr, Phys. Rev. Lett. **27**, 654 (1971).
- ¹⁷A. F. G. Wyatt, N. A. Lockerbie, and R. A. Sherlock, Phys. Rev. Lett. **33**, 1425 (1974).
- ¹⁸I. M. Khalatnikov, *An Introduction to the Theory of Superfluidity* (Addison-Wesley, Redwood City, CA, 1989).
- ¹⁹A. F. G. Wyatt, M. A. H. Tucker, I. N. Adamenko, K. E. Nemchenko, and A. V. Zhukov, Phys. Rev. B **62**, 3029 (2000).
- ²⁰I. N. Adamenko, K. E. Nemchenko, and A. F. G. Wyatt, Low Temp. Phys. **29**, 11 (2003) [Fiz. Nizk. Temp. **29**, 16 (2003)].
- ²¹I. N. Adamenko, K. E. Nemchenko, V. A. Slipko, and A. F. G. Wyatt, Phys. Rev. B **68**, 134507 (2003).
- ²²I. N. Adamenko, K. E. Nemchenko, V. A. Slipko, and A. F. G. Wyatt, J. Low Temp. Phys. **138**, 67 (2005).
- ²³I. N. Adamenko, Yu. A. Kitsenko, K. E. Nemchenko, V. A. Slipko, and A. F. G. Wyatt, Fiz. Nizk. Temp. **31**, 607 (2005) [Low Temp. Phys. **31**, 459 (2005)].